Published online 27 August 2018

Nucleic Acids Research, 2018, Vol. 46, No. 19 ***10119–10131***
doi: 10.1093/nar/gky775

Nucleolar residence of the seckel syndrome protein TRAIP is coupled to ribosomal DNA transcription

Yangzi Chen[1], Junshi Li[1], Fakun Cao[1], Jason Lam[1], Clooney C.Y. Cheng[1], Cheng-han Yu[1,*] and Michael S.Y. Huen[1,2,3,*]

[1]School of Biomedical Sciences, LKS Faculty of Medicine, The University of Hong Kong, Hong Kong S.A.R., [2]Center for Synthetic Biology Engineering Research, Shenzhen Institutes of Advanced Technology, Chinese Academy of Sciences, Shenzhen 518055, PR China and [3]State Key Laboratory of Brain and Cognitive Sciences, The University of Hong Kong, Hong Kong S.A.R.

Received May 06, 2018; Revised August 10, 2018; Editorial Decision August 14, 2018; Accepted August 16, 2018

ABSTRACT

The RING finger protein TRAIP protects genome integrity and its mutation causes Seckel syndrome. TRAIP encodes a nucleolar protein that migrates to UV-induced DNA lesions via a direct interaction with the DNA replication clamp PCNA. Thus far, mechanistically how UV mobilizes TRAIP from the nucleoli remains unknown. We found that PCNA binding is dispensable for the nucleolus-nucleoplasm shuttling of TRAIP following cell exposure to UV irradiation, and that its redistribution did not rely on the master DNA damage kinases ATM and ATR. Interestingly, I-PpoI-induced ribosomal DNA damage led to TRAIP exclusion from the nucleoli, raising the possibility that active ribosomal DNA transcription may underlie TRAIP retention in the nuclear sub-compartments. Accordingly, chemical inhibition of RNA polymerase I activity led to TRAIP diffusion into the nucleoplasm, and was coupled with marked reduction of DNA/RNA hybrids in the nucleoli, suggesting that TRAIP may be sequestered via binding to nucleic acid structures in the nucleoli. Consistently, cell pre-treatment with DNase/RNase effectively released TRAIP from the nucleoli. Taken together, our study defines a bipartite mechanism that drives TRAIP trafficking in response to UV damage, and highlights the nucleolus as a stress sensor that contributes to orchestrating DNA damage responses.

INTRODUCTION

The eukaryotic nucleus is highly compartmentalized and houses a vast number of cytologically discernable nuclear bodies, including the nucleolus (1). Aside serving as the dedicated site for ribosomal RNA (rRNA) synthesis, pre-rRNA processing and ribosome subunit assembly, the nucleolus has evolved to couple ribosome biogenesis with cellular stress detection and response, and is emerging as a protein hub that orchestrates diverse biological processes, including cell cycle checkpoint control and DNA repair (2,3). Current evidence indicates that cellular stress signals, including those that arise from nutrient deprivation, hypoxia and DNA damage, converge to inhibit RNA polymerase I activity, thereby suppressing rRNA synthesis (4). Mechanistically how cellular stress signals reach the nucleolus is only beginning to unfold, although nucleolus stress response coincides with structural re-organization of the nucleolus, and entails the dynamic flux of proteins in and out of the nucleolar compartments (2,5). Importantly, genetic mutations that perturb nucleolar integrity or function are causally associated with human diseases (6–9), and recent studies are also uncovering intimate relationships between cell proliferation status with size and number of nucleoli (10–13).

Although advanced proteomics technologies have led to the identification of an extensive list of human proteins in the nucleolus (14,15), the fundamental bases that dynamically regulate their occupancy in the non-membrane bound organelle have remained an area of research interest (16). While previous studies suggested that nucleolar import can be mediated by short stretches of basic amino acids (lysines and arginines) (17,18), it is becoming evident that nucleolar targeting can also be regulated via physical interactions with core nucleolar proteins and rDNA (19). Moreover, spatial confinement of nucleolus-residing factors is highly dynamic, and is amenable to regulation via sophisticated signal transduction events (16).

The RING finger protein TRAIP (a.k.a. RNF206) promotes genome stability (20–27) and is mutated in patients with microcephalic primordial dwarfism (Seckel syndrome) (24). While human TRAIP encodes a nucleolus-residing protein, recent evidence has established TRAIP as a key

*To whom correspondence should be addressed. Tel: +852 39176868; Fax: +852 28170857; Email: huen.michael@hku.hk
Correspondence may also be addressed to Cheng-han Yu. Tel: +852 39179205; Fax: +852 28170857; Email: chyu1@hku.hk

component of the mammalian replicative stress response (22,24,25,27,28). Indeed, TRAIP enforces genome duplication by promoting the recovery of stressed replication forks and the resumption of DNA replication following UV damage. This is accomplished by its ability to dock at UV-induced DNA lesions via a direct interaction with the DNA replication clamp PCNA (22,25), although exactly how TRAIP is released from the nucleolus remains unknown. Moreover, the observations that 5′ epitope tagging and genetic mutations that target its N-terminal RING excluded TRAIP from the nucleolus and adversely interfered with cell proliferation and organismal development underscore nucleolar retention as a pivotal regulatory mechanism that contributes to its functionality as a replicative stress response protein (22,24–26).

MATERIALS AND METHODS

Antibodies and chemicals

The anti-TRAIP polyclonal antibodies were raised against GST tagged TRAIP-N terminal fusion proteins and were affinity-purified using column coated with N-terminal MBP tagged TRAIP as previously described (29). Anti-γH2AX antibodies were previously described (30). The anti-S9.6 antibodies were from Kerafast (Boston, USA); anti-Nucleolin (C23) antibodies were from Santa Cruz (Dallas, TX, USA); anti-Ki67 antibodies were from Chemicon (Darmstadt, Germany). (*Z*)-4-Hydroxytamoxifen (4-OHT), anti-Actin, anti-Flag (Rabbit) and anti-Flag (Mouse; Clone M2) antibodies were from Sigma (Darmstadt, Germany); anti-pRPA32 antibodies were from Bethyl Laboratories. Shield-1 was purchased from Takara (Kanagawa, Japan). Hydroxyurea, Aphidicolin, Mitomycin C, Cisplatin, Actinomycin D, α-Amanitin, and DRB were from Sigma (Darmstadt, Germany). CX5461, ATM inhibitor (ATMi; KU55933) and ATR inhibitor (ATRi; VE821) were from SelleckChem (Houston, TX, USA). DAPI (4′,6-diamidino-2-phenylindole) and DNase I (EN0523) was from Thermo Fisher Scientific. RNase A was from Qiagen.

Construction of TRAIP expression plasmids

For all the epitope-tagged TRAIP expression constructs (wild type and mutants), cDNAs were subcloned into pDONR201 vectors using Gateway technology (Invitrogen), and were subsequently transferred to Gateway-compatible destination vectors for bacterial or mammalian expression. Mutagenesis was performed by PCR and all constructs were verified by sequencing. To determine the subcellular localization of Flag epitope-tagged TRAIP (TRAIP-Flag) proteins in U2OS cells, TRAIP was expressed from the TRAIP-SFB plasmid (Addgene Plasmid #101769) as described previously (25). Likewise, all TRAIP variants carrying C-terminal Flag epitopes were expressed essentially as full-length TRAIP-Flag.

Cell culture and stable cell generation

U2OS and HeLa cells were cultured in DMEM supplemented with 10% FBS at 37°C in 5% CO_2. For the generation of cell lines with ectopic expression of TRAIP alleles, BOSC23 cells were transfected with retroviral-based expression constructs together with pCL-Ampho using polyethyleneimine (PEI; Polysciences Inc., Warrington, USA). Viral supernatants were collected and filtered 48 and 72 h after transfection and were subsequently applied to recipient cells. Stable cells were selected in the presence of 2 μg/ml puromycin-supplemented culture medium.

Immunostaining procedure

Unless otherwise stated, cells grown as monolayers on coverslips were fixed in 3% paraformaldehyde at room temperature for 15 min, followed by permeabilization with 0.5% Triton X-100 solution for 10 s. Nuclei were visualized by staining with DAPI. Images were acquired using an Olympus BX51 fluorescence microscope (Tokyo, Japan). For ATM/ATR inhibition experiments, cells grown on coverslips were pre-incubated with ATM inhibitor KU55933 or ATR inhibitor VE821 for 3 h. Cell culture media were aspirated for UV treatment (UVC; Spectrolinker™ XL-1000 Series), but were re-applied to cells in the presence of the respective kinase inhibitors during cell recovery. Cells were fixed and processed for immunofluorescence staining 4 h post UV treatment.

Photobleaching and photo-switching experiments

Point-photobleaching experiments of TRAIP-GFP expressing U2OS cells were performed on an inverted confocal microscope with a live cell incubator at 37°C (Perkin Elmer UltraView VOX, Waltham, MA, USA). Cells were imaged with a 100 × 1.45 oil objective and a Hamamatsu C9100-23B EMCCD Camera at 0.2-s intervals. Five images were taken before the bleaching application. ImageJ was used to calculate and normalize fluorescence intensity at ROIs, and the fluorescence recovery curves were generated using Prism (GraphPad Software) with each data point representing mean ± SEM. Photo-switchable TRAIP-mEOS2 construct was generated by subcloning TRAIP cDNA into the mEOS2-N1 vector, a gift from Michael Davidson and Loren Looger (Addgene #54662) (31). Photo-switching experiments were performed on a spinning disk microscope with a 405nm (50mW) laser and a live cell incubator at 37°C (Perkin Elmer UltraView VOX, Waltham, MA, USA). TRAIP-mEOS2 expressing U2OS cells were imaged by 488 nm (40 mW) laser excitation and were photo-switched by a single 405nm laser point activation. Immediately, photo-switched TRAIP-mEOS2 were imaged by 561 nm (50 mW) laser excitation at 0.2-s intervals on a Hamamatsu C9100-23B EMCCD camera. Images from the photo-switching experiments were captured using Volocity (Perkin Elmer, Waltham, MA, USA). Raw intensities at ROIs were calculated using ImageJ and the time-intensity plots were generated by Prism (GraphPad Software).

In vitro DNase/RNase digestion

Epitope-tagged TRAIP-expressing U2OS cells were grown on coverslips and were subsequently permeabilized with 0.5% Triton X-100 in PBS for 80 s as described (32). Cells were washed briefly with solution buffer [20 mM HEPES

(pH 7.4), 50 mM NaCl, 3 mM $MgCl_2$ and 300 mM sucrose], and were subsequently treated with RNase A (1 mg/ml) or DNase I (0.5 U/μl), or buffer alone for 1 h at 37°C. Cells were fixed thereafter with 3% PFA for 20 min at RT and were subjected to immunofluorescence staining experimentations.

Statistical analysis

For multiple group comparisons, data were subjected to one-way ANOVA followed by Dunnett's *t*-test for those that yielded significance in the ANOVA test. For comparison between test and control groups, Student's *t*-test was performed. Significance was reported starting at $P < 0.05$.

RESULTS

TRAIP trafficking in response to UV irradiation

TRAIP responds to UV irradiation by shuttling from the nucleoli to γH2AX-marked DNA lesions (22,24,25) (Supplementary Figure S1A). The ability of TRAIP to concentrate at UV-induced DNA lesions depends on its C-terminal PIP motif, which mediates a direct interaction with the DNA replication clamp PCNA (22,25). Because TRAIP concentrates in the nucleoli, to understand how TRAIP is mobilized in response to UV damage, we attempted to separate the sequence of events that regulate the nucleolus-nucleoplasm shuttling of TRAIP from its ability to accumulate at UV-induced DNA lesions. To this end, we expressed TRAIP and its PIP mutant (TRAIP-PIP*) in U2OS cells as fusion proteins by epitope-tagging a Flag sequence at their C-terminus in order to preserve their native nucleolar localization (Figure 1A and Supplementary Figure S1B). Consistent with previous reports, UV irradiation relocalized TRAIP-Flag from the nucleoli and led to its accumulation at γH2AX foci, and that TRAIP-Flag accumulation at γH2AX foci was strictly dependent on its PIP motif (Figure 1B) (22,25). Although TRAIP-Flag was expressed at a higher level when compared to endogenous TRAIP (Supplementary Figure S1C), it retained the ability to dock at UV-induced DNA lesions, as TRAIP-Flag extensively colocalized with γH2AX foci (Figure 1B) as well as phospho-RPA foci (Supplementary Figure S1D) following cell exposure to UV irradiation. Importantly, although TRAIP-PIP* did not accumulate into foci structures, we found that the mutant TRAIP proteins were dispersed into the nucleoplasm following UV treatment (Figure 1B). This supported the idea that TRAIP trafficking in response to UV damage may be regulated by a two-step mechanism, in which UV triggers the nucleolus-nucleoplasm redistribution of TRAIP prior to its PIP-dependent accumulation at stressed replication forks (Figure 1C). If this model were correct, we posit that mutations that mis-localize TRAIP from the nucleoli may still accumulate at UV-induced DNA lesions. Indeed, although the C-terminal half of TRAIP (C-Flag) did not localize in the nucleoli, it retained the ability to concentrate into UV-induced foci (Figure 1D). Similar to the requirement of the PIP motif in the context of full-length TRAIP, mutating the PIP motif on C-Flag (C-PIP*-Flag) compromized its ability to concentrate into γH2AX foci (Figure 1D).

Noting that human TRAIP mutations were recently identified in patients with microcephalic primordial dwarfism (24), we also sub-cloned the two TRAIP alleles, namely R185X and R18C, and explored how the mutations may affect the sub-cellular localization of TRAIP. Intriguingly, in stark contrast to full-length TRAIP, both R18C and R185X were excluded from the nucleoli (Figure 1E). We also tested whether the human TRAIP mutations may dysregulate their responsiveness to UV irradiation. Because R185X was expressed predominantly in the cytoplasm (Figure 1E), we fused R185X to the SV40 Large T antigen-derived nuclear localization sequence (NLS; PKKKRKV) to ensure that it resides in the nuclear compartment. Interestingly, we found that R185X-NLS resides predominantly in the nucleoli, was dispersed into the nucleoplasm in response to UV, but failed to concentrate at UV-induced foci (Figure 1F). On the other hand, although it did not properly localize in the nucleoli, TRAIP R18C docked at UV-induced DNA lesions (Figure 1F). The observation that R18C, which targeted the TRAIP RING domain, did not localize in the nucleoli is in line with previous reports where mutations of the TRAIP RING domain, either by point inactivation of the conserved cysteine (C7A) or its deletion, perturbed nucleolar occupancy of TRAIP (25). Together, we concluded that the nucleolus-nucleoplasm redistribution of TRAIP is distinctly regulated, and can be separated from the PIP-dependent concentration of TRAIP at UV-induced DNA lesions.

Dynamic nucleolus-nucleoplasm shuttling of TRAIP

Previous studies have documented that residence of nucleolar proteins is highly dynamic (14,15,33), and that their nucleolar residence time is determined by their affinities for nucleolar elements, including ribosomal DNA/RNA and core nucleolar proteins (34). To examine the nucleolus-nucleoplasm shuttling of TRAIP, we expressed TRAIP in frame with the cDNA that encodes the photo-convertible fluorescent protein mEOS2. mEOS2 can be photo-converted using a 405 nm laser, and can be monitored by excitation with a 561 nm laser (35). Consistent with its native localization, TRAIP-mEOS2 predominantly resides in the nucleoli in U2OS cells (Figure 2A-B). Accordingly, photo-conversion of nucleoplasmic TRAIP-mEOS2 with a 405nm laser led to a swift increase of photo-converted TRAIP-mEOS2 in the nucleoli (Figure 2B and C; Zone 1). By contrast, photo-converted TRAIP-mEOS2 was below detection limit in the nucleoplasm throughout our experimentations (Figure 2B and C; Zone 2). The fact that signals from photo-converted TRAIP-mEOS2 inside the nucleolus (Zone 1) gradually declined in between laser pulses suggests that TRAIP is dynamically mobilized (Figure 2C), and highlights that TRAIP, in reminiscence to many nucleolar factors, shuttles bi-directionally between the nucleoli and the nucleoplasm (33).

Mapping of nucleolar retention signals on the TRAIP polypeptide

To understand how TRAIP is retained in the nucleoli, we attempted to experimentally map the nucleolar reten-

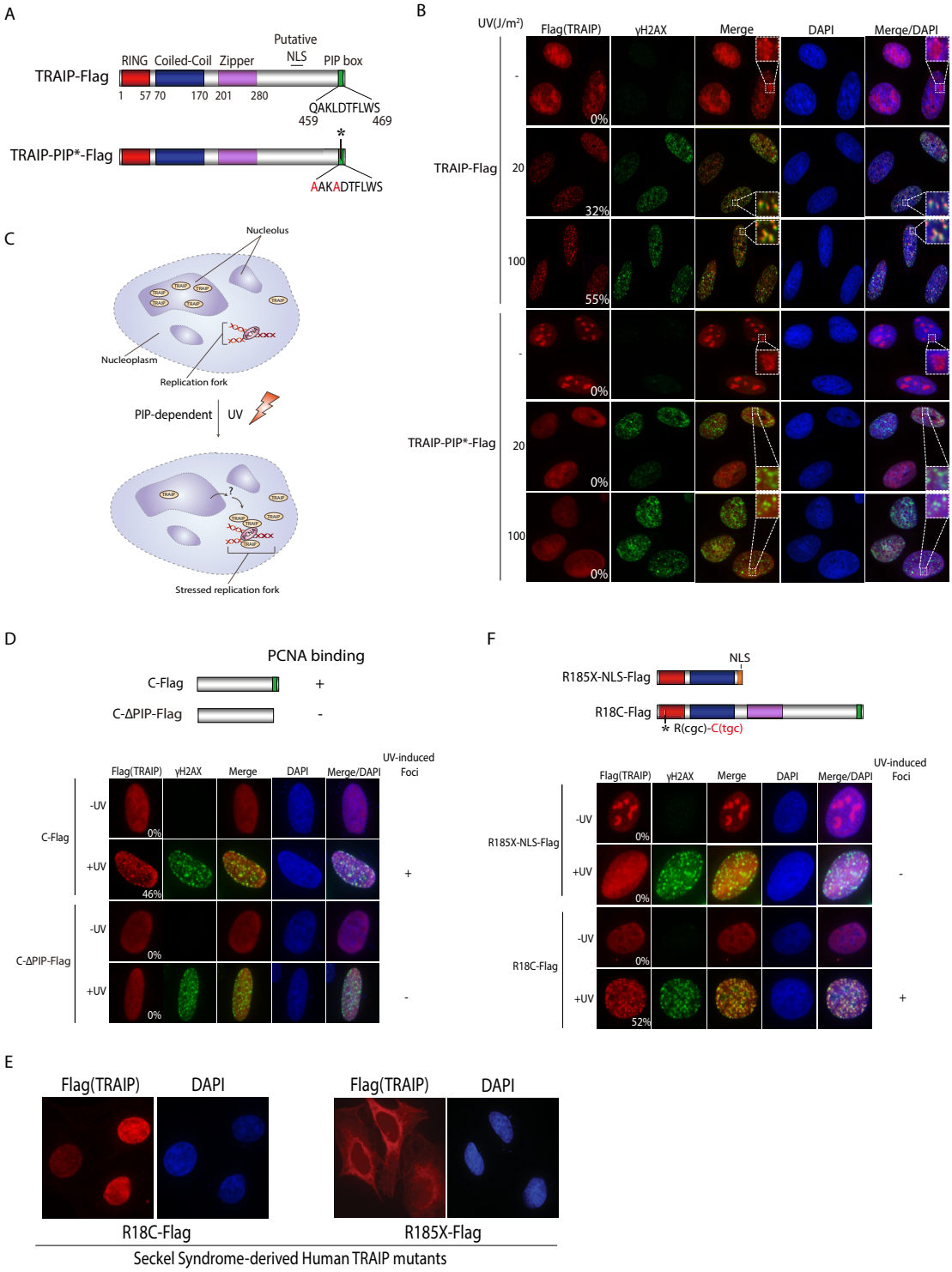

Figure 1. UV triggers a global redistribution of TRAIP in the cell nuclei. (**A**) Schematic illustration of TRAIP protein and its domain organization. TRAIP bears a C-terminal PCNA-Interacting Protein (PIP) motif. NLS; nuclear localization sequence. (**B**) Redistribution of TRAIP in response to UV irradiation. Cells expressing TRAIP-Flag or its PCNA binding-defective PIP mutant (TRAIP-PIP*-Flag) were subjected to increasing doses of UV. Cells were subsequently processed for immunostaining experiments. γH2AX was used as a DNA damage marker. Nuclear DNA was visualized using DAPI. Percentage of cells with UV-induced TRAIP foci are shown. (**C**) Proposed model depicting TRAIP redistribution following cell exposure to UV irradiation (see text). (**D**) Schematic illustration of TRAIP C terminus (top panel). Cells expressing TRAIP C terminus (C-Flag) or its PCNA binding-defective counterpart (C-ΔPIP-Flag) were treated with UV before they were processed for immunostaining experiments as described for (B). Percentage of cells with UV-induced TRAIP foci are shown. (**E**) Patient-derived TRAIP mutations, namely R18C and R185X, were expressed in U2OS cells. Cells were processed as in (B) to visualize the subcellular localization of mutant TRAIP proteins. (**F**) Schematic illustration of Seckel syndrome-derived TRAIP mutations (top panel). Cells expressing TRAIP mutant proteins were processed for immunostaining experiments as in (B). Percentage of cells with UV-induced TRAIP foci are shown. All quantifications are derived from at least 3 independent experiments and more than 100 cells were scored.

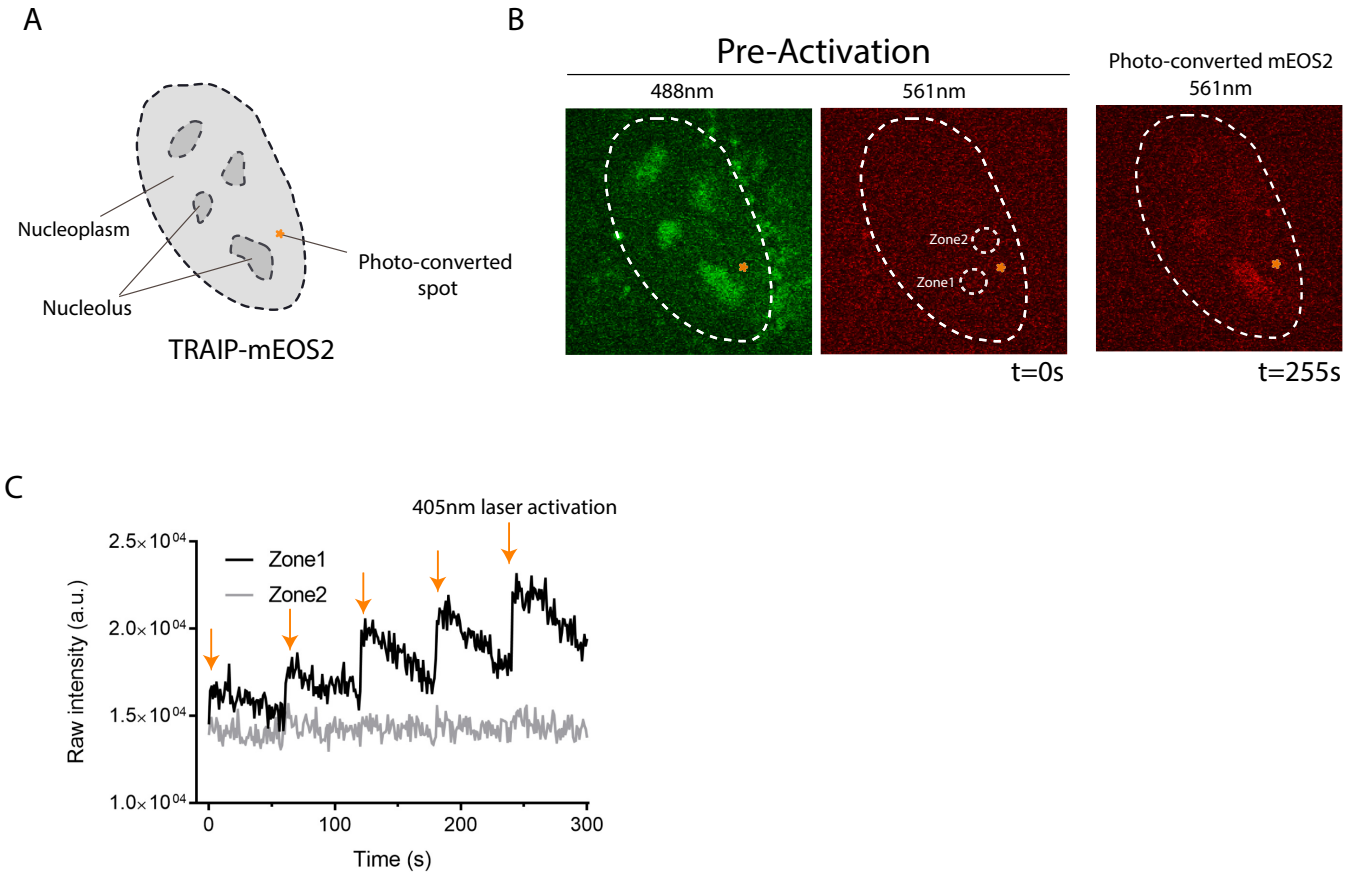

Figure 2. Rapid exchange of nucleolar TRAIP proteins. (**A**) The star marked the 405nm laser applying region. Zone 1 and Zone 2 were selected based on their equal distance from the activation site (i.e. photo-converted spot). (**B** and **C**) Time-lapse images were taken of Zone 1 and Zone 2 at 0.2-s intervals. After five times of activation, predominant TRAIP-mEOS2 accumulated in Zone 1, whereas negligible amount of TRAIP-mEOS2 can be observed in Zone 2. Quantification of the fluorescence intensity in Zone 1 and Zone 2 is displayed (**C**). Orange colored arrows indicate each activation event.

tion signal(s) on TRAIP. To this end, we ectopically expressed a panel of TRAIP alleles (Supplementary Figure S2), and examined their sub-cellular localization by indirect immunofluorescence staining experiments (Figure 3A). These experiments were performed in both PFA fixed cells as well as in cells pre-extracted with a 0.5% triton solution, a standard procedural step that removes the 'soluble' protein pool to better reveal protein sub-cellular localization. Because the putative NLS resides on the C terminal half of the TRAIP polypeptide (residues 395–405; GQKQPK RPRSE), the SV40 Large T-antigen-derived NLS sequence was fused to TRAIP alleles that lacked this region (Figure 3A). Consistent with the predicted location of the TRAIP NLS, the C terminal half of TRAIP (C-Flag) resided in the nucleus, despite its inability to concentrate in the nucleoli (Figure 3B and C). Moreover, C-Flag was readily extracted by 0.5% Triton solution, suggesting that it was not tethered to any nuclear compartments. By contrast, not only did we find that the TRAIP N terminal fragment (N-NLS-Flag) concentrated in the nucleoli, but its ability to do so appeared to be more efficient than full-length TRAIP proteins (Figure 3B and C). In addition, we found that deleting either the Coiled-coil domain (ΔCC-Flag) or the Zipper (ΔZip-Flag) domain resulted in modest reduction of TRAIP accumulation in the nucleoli, and that the compound mutant lacking both the Coiled-coil and Zipper domains (ΔCC-Zip-Flag) was excluded from the nucleoli (Figure 3B and C). Similar to C-Flag, ΔCC-Zip-Flag proteins were also readily extracted by Triton solution. Together, these data suggest that the Coiled-coil and Zipper domains may act in concert to target TRAIP into the nucleoli.

To explore whether the Coiled-coil and Zipper domains may be sufficient to target TRAIP into the nucleoli, we expressed these otherwise cytoplasmic proteins in frame to the NLS peptide (Figure 3A). Interestingly, upon Triton pre-extraction, we found that the Zipper domain (Zip-NLS-Flag) alone or in combination with the Coiled-coil sequence (CC-Zip-NLS-Flag) supported nucleolar residence at comparable levels to full-length TRAIP proteins (Figure 3D and E). On the other hand, the majority of the Coiled-coil fragment (CC-NLS-Flag) did not properly concentrate in the nucleoli (Figure 3D). Moreover, unlike the nucleolar marker Nucleolin and TRAIP protein fragments that resided predominantly in the nucleoli, we noted that CC-NLS-Flag proteins were not resistant to 0.5% Triton pre-extraction, suggesting that the Coiled-coil domain did not stably associate with nucleoli structures. Together, these data suggest

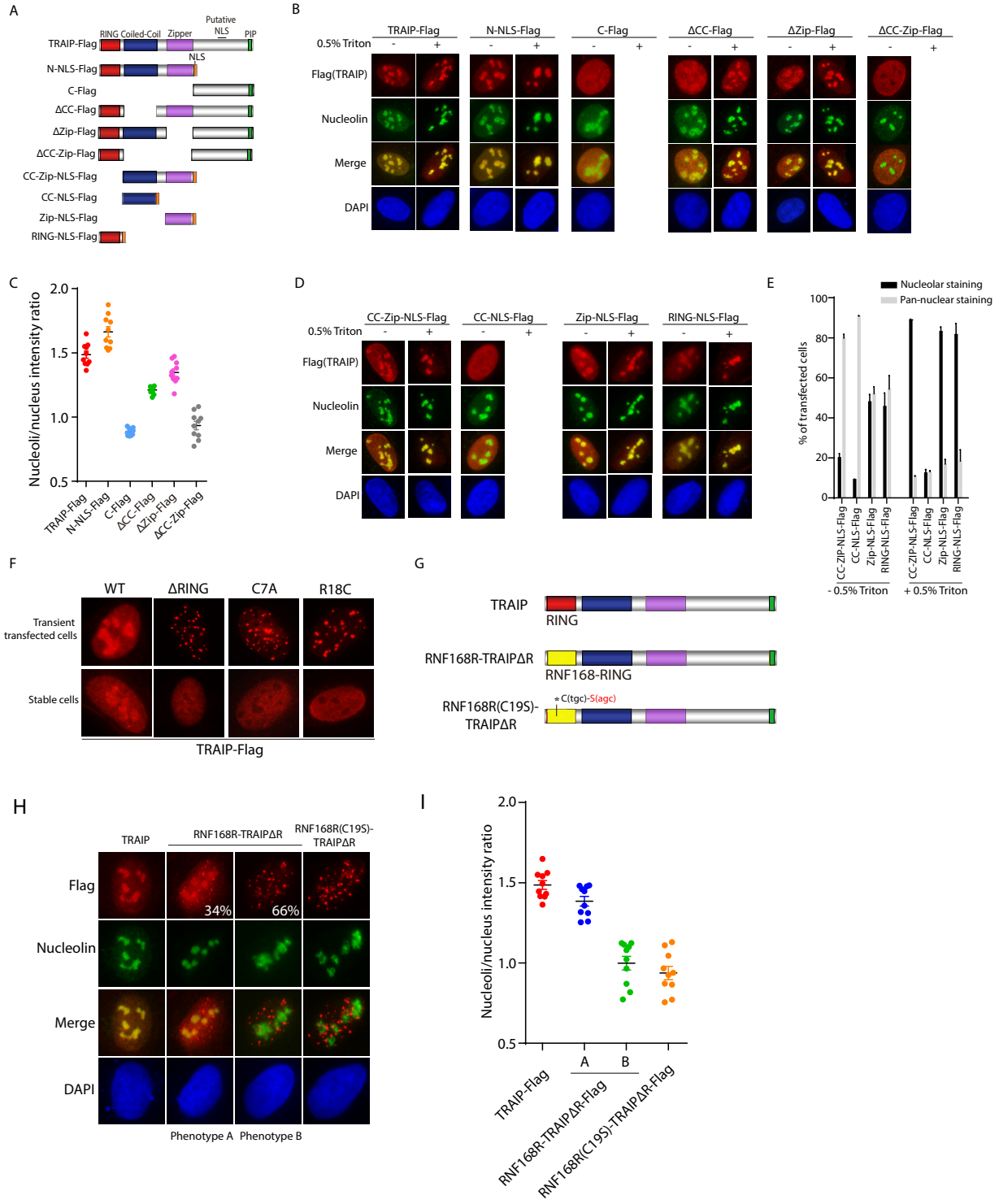

Figure 3. Nucleolar targeting of TRAIP requires its N terminus. (**A**) Schematic illustration of TRAIP and its alleles. NLS; nuclear localization signal. (**B–E**) Representative images showing the subcellular localization of TRAIP and its alleles in U2OS cells. Cells were transfected with TRAIP expression plasmids and were incubated with or without Triton pre-extraction (0.5% Triton) prior to processing for immunostaining experiments using indicated antibodies. Nucleolin was used as a nucleolar marker, whereas nuclear DNA is visualized by DAPI staining. Note that C-Flag and ΔCC-Zip-Flag proteins were readily extracted by 0.5% Triton solution, and were not detectable (see text). The nucleoli/nucleus intensity ratio of (B) was calculated by ImageJ, $n = 10$ (C). Percentage of cells (mean±SEM) exhibiting pan-nuclear and nucleolar signals from (D) were plotted (E). (**F**) Representative images showing the subcellular localization of TRAIP and its RING mutants in transiently transfected cells (upper row) and in cells that have been selected for stable expression (bottom row). (**G**) Schematic illustration showing the construction of chimeric RING fusion proteins. (**H–I**) Representative images showing the subcellular localization of TRAIP and the chimeric RING fusion proteins. Immunostaining experiments were performed as described in (B). Percentage of RNF168R-TRAIPΔR-expressing cells exhibiting each of the two distinct sub-cellular localization (i.e. Phenotype A & Phenotype B) is shown. The nucleoli/nucleus intensity ratio of TRAIP proteins in U2OS cells (H) was calculated by ImageJ and are shown, $n = 10$ (I).

that the Zipper domain may play an important role in mediating TRAIP retention in the nucleoli.

TRAIP harbours a RING domain at its N-terminus (Figure 1A), and mutations that target its RING domain, including the C7A and RING-deletion mutations, have been shown to perturb its nucleolar residence (25) (Figure 3F). Moreover, the Seckel syndrome-derived TRAIP R18C mutation also impaired the ability of TRAIP to reside in the nucleoli (Figures 1E–F and 3F). It is noteworthy to mention that TRAIP RING mutants display a tendency to aggregate and form speckle-like structures in the nuclei when they are expressed at high levels (Figure 3F), as in the case in transiently transfected cells or in cells pre-treated with the proteasome inhibitor MG132 (25). While RING-NLS-Flag also enriched in the nucleoli (Figure 3D and E), to further study the contribution of TRAIP RING in mediating its nucleolar residence, we replaced the TRAIP RING with the RNF168 RING, and examined the sub-cellular localization of the RNF168 RING-TRAIPΔRING chimeric proteins (Figure 3G). We posit that if the TRAIP RING domain were important in mediating its concentration in the nucleoli, its replacement with RNF168 RING should not support nucleolar localization, as RNF168 does not reside in the nucleoli (36). Accordingly, we found that a substantial fraction of the RNF168 RING-TRAIP chimeric fusion proteins were mis-localized, which was further exacerbated by the RING-inactivating C19S mutation (Figure 3H-I). These observations suggest that TRAIP RING may also be important in mediating its nucleolar retention, and that the E3 ubiquitin ligase signature motif on TRAIP may be endowed with specialized function in regulating its intracellular compartmentalization.

Nucleolar dynamics of TRAIP proteins

To examine the dynamic nucleolus-nucleoplasm shuttling of TRAIP, we conducted photo-bleaching experiments on TRAIP-GFP proteins in live U2OS cells. Consistent with its native subcellular distribution, TRAIP-GFP resided predominantly in the nucleoli, with a small fraction diffusely localized in the nucleoplasm (Figure 4A). We irreversibly quenched GFP signals in either the nucleoplasm (Zone 1) or the nucleolus (Zone 2), and monitored cells by time-lapse confocal microscopy. Accordingly, we found that recovery of GFP signals in both photobleached areas was rapid (Figure 4B and C), suggesting that TRAIP is dynamically exchanged between the nucleoplasmic and nucleolar compartments. The fact that nucleolar TRAIP-GFP proteins did not fully recover within the time frame of our analysis suggests that a fraction of TRAIP-GFP may be relatively immobile.

Our observations that both TRAIP RING and Zipper domains may play important roles in mediating nucleolar residence of TRAIP proteins (Figure 3D and E) prompted us to further study the dynamics of TRAIP RING and Zipper domains in the nucleoli. To this end, we expressed RING-NLS-GFP or Zip-NLS-GFP in U2OS cells (Figure 4D), and performed photo-bleaching experiments essentially as described for TRAIP-GFP (Figure 4A–C). We also included R185X-NLS-GFP, as this Seckel syndrome-derived TRAIP mutant allele was proficient in mediating its nucleolar enrichment (Figures 1F and 4D). Intriguingly, we found that recovery of GFP signals was robust, and that RING-NLS-GFP, Zip-NLS-GFP and R185X-NLS-GFP recovered with much faster kinetics when compared to full-length TRAIP-GFP proteins (Figure 4E-F). These data support the idea that TRAIP RING and Zipper domains may, in concerted effort, mediate TRAIP enrichment in the nucleoli.

UV-induced TRAIP mobilization is independent of the DDR kinase ATM / ATR

Given the established roles of the DNA Damage Response kinases ATM and ATR in mounting UV-induced DNA damage responses (37,38), we next explored whether the ATM/ATR kinases may regulate TRAIP release from the nucleoli. To this end, we took advantage of commercially available small molecules, namely KU55933 and VE821, that have been extensively characterized in their specificity for inhibiting ATM and ATR activities, respectively (39). Importantly, pre-treatment of KU55933 (ATMi) or VE821 (ATRi) alone or in combination did not noticeably affect TRAIP residence in the nucleoli in unperturbed cells, nor did it impair its ability to mobilize to UV-induced foci (Figure 5A–C), although chemical inhibition of ATM/ATR resulted in significant reduction of cells positively stained by anti-γH2AX antibodies (Figure 5A and B).

UV irradiation inhibits ribosomal RNA (rRNA) synthesis. To document the effect of UV irradiation on rDNA transcription, we immunostained control and UV-treated cells with S9.6 antibodies, which specifically recognize DNA–RNA hybrids (R-loops). In line with previous reports, S9.6 signals are enriched in the nucleoli (40,41) (Supplementary Figure S3A), but can also be observed in the cytoplasm in unperturbed cells (41,42). Strikingly, UV treatment led to substantial reduction of nucleolar S9.6 signals in a manner that did not correlate with γH2AX status (Supplementary Figure S3A and B). In support of the dispensable role of the DDR kinases, nucleolar S9.6 staining pattern and intensity were indistinguishable among cells pre-treated with the ATM/ATR-specific inhibitors in comparison to control (Figure 5D and E). These data argue that UV triggers TRAIP redistribution in an ATM/ATR-independent manner, and highlight the possibility that TRAIP retention in the nucleoli may be coupled to rDNA transcriptional processes.

Inhibition of ribosomal RNA synthesis releases TRAIP from the nucleoli

To evaluate how genotoxic stress may couple TRAIP redistribution and R-loop dynamics, we determined the subcellular localization of epitope-tagged TRAIP in U2OS cells following treatment of a panel of DNA damaging agents (Figure 6A). Intriguingly, although DNA damage-induced γH2AX foci were evident, in contrast to other DNA damaging agents, we found that UV irradiation was most effective in fueling robust TRAIP-Flag accumulation at γH2AX foci (Figure 6A) and in suppressing nucleolar S9.6 signals (Figure 6B), suggesting that nucleolar release of TRAIP may be coupled to R-loop dissolution following UV irradiation. Importantly, although UV irradiation triggered robust

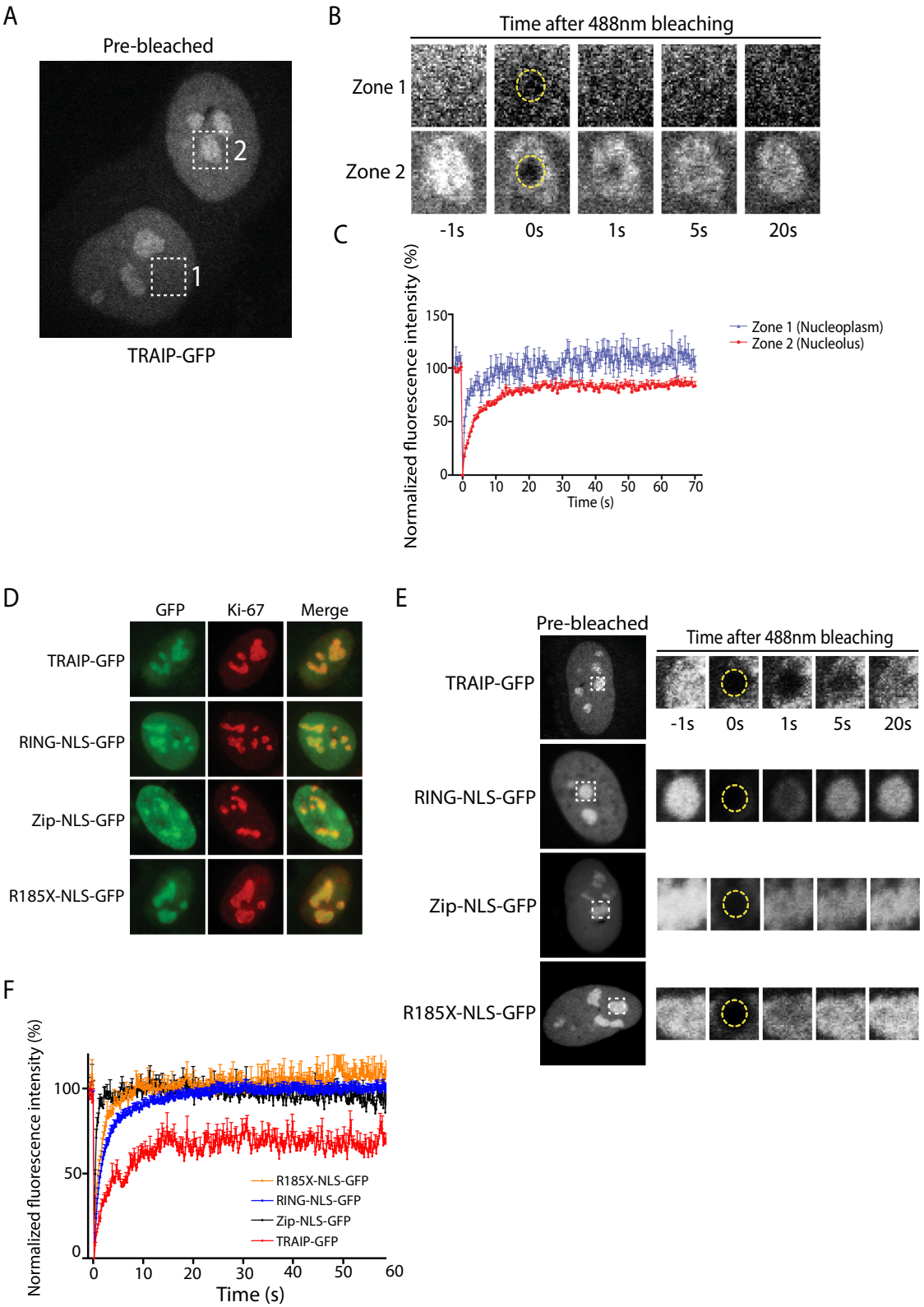

Figure 4. TRAIP dynamically associates with the nucleoli. (**A**) TRAIP-GFP resides predominantly in the nucleoli in U2OS cells. The 488nm laser was applied to Zone 1 in the nucleoplasm and Zone 2 in the nucleolus of TRAIP-GFP-expressing U2OS cells. (**B** and **C**) Live cell time-lapse images pre and post photo-bleaching were taken by a Perkin Elmer UltraView VOX spinning disk microscope. The recovery lines were generated from quantification of 20 cells (**C**); (**D**) TRAIP-GFP and its alleles colocalized with the nucleolar marker Ki-67; (E–F) TRAIP-GFP and its alleles were expressed and monitored in live U2OS cells as in (A). Note that cells exhibiting nucleolar enrichment of each of the TRAIP-GFP proteins were selected for experimentations. Live cell time-lapse images pre and post photo-bleaching were taken at indicated time points (**E**). The recovery lines were generated from quantification of five cells (**F**).

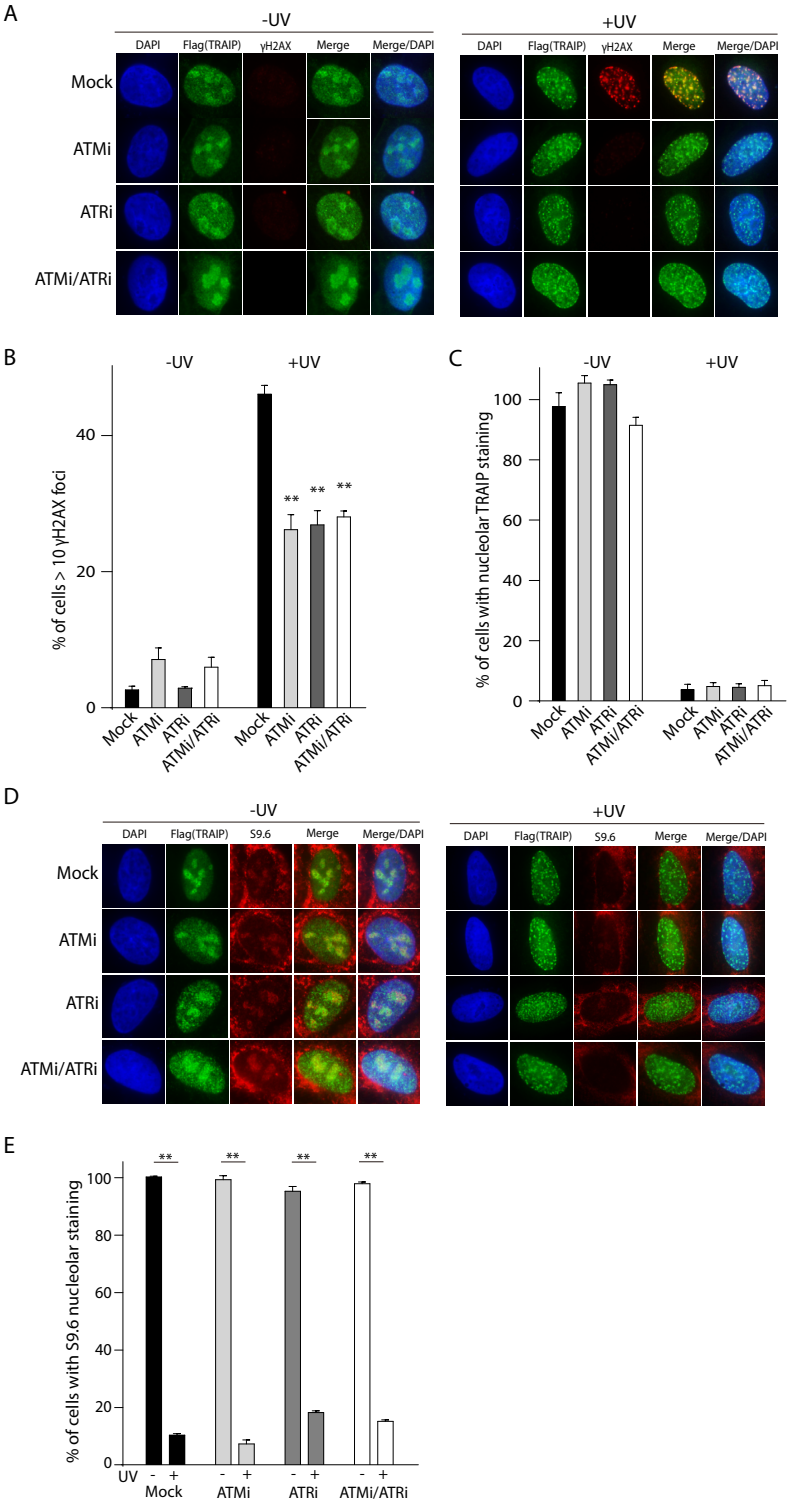

Figure 5. ATM/ATR-independent nucleolar release of TRAIP in response to UV. (**A**–**C**) Chemical inhibition of ATM and ATR did not suppress UV-induced TRAIP accumulation at γH2AX sites. Cells engineered to stably express TRAIP-Flag were pre-treated with ATM- or/and ATR-specific inhibitors for 3 h prior to their exposure to UV irradiation (100 J/m^2). Cells were fixed and processed for immunostaining experiments using indicated antibodies 4 h post UV treatment. γH2AX was used as a DNA damage marker. Nuclear DNA was visualized using DAPI. Both ATMi (KU55933) and ATRi (VE821) were used at a final concentration of 10 μM. Quantification of cells with more than 10 γH2AX foci (**B**) and with prominent nucleolar TRAIP-Flag signals (**C**) are shown. Results (mean±SEM) were derived from 3 independent experiments and at least 100 cells were scored. $^{**}P < 0.01$ versus Mock; (**D** and **E**) UV exposure dissolved nucleolar R-loops in an ATM/ATR-independent manner. TRAIP-Flag-expressing U2OS cells subjected to UV treatment were fixed 4 h after, and were processed for immunostaining experiments using indicated antibodies. S9.6 antibodies stain DNA/RNA hybrids (i.e. R-loops). Quantification of cells (mean ± SEM) with nucleolar S9.6 signals is shown (E) and were derived from 3 independent experiments, $n > 100$. $^{**}P < 0.01$ versus no UV.

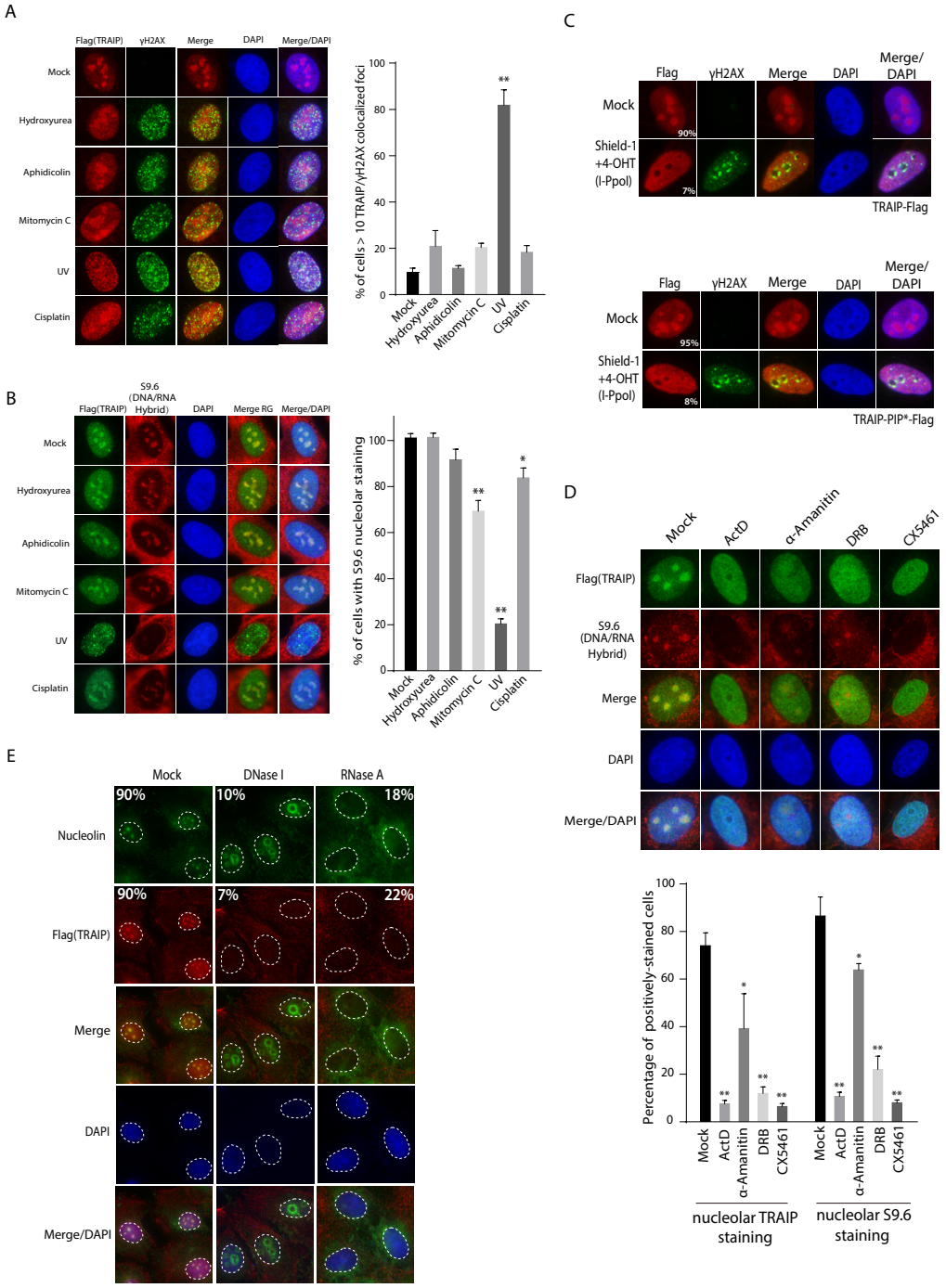

Figure 6. R-loop dissolution is coupled to TRAIP redistribution. (**A** and **B**) U2OS cells that stably express TRAIP-Flag were subjected to a panel of DNA damaging agents. Cells were subsequently fixed and processed for immunostaining experiments using indicated antibodies. Dose and duration of treatment were empirically determined to yield similar number and intensity of γH2AX foci: Hydroxyurea (5 mM, 4 h); Aphidicolin (5 μM, 4 h); Mitomycin C (1 μM, 4 h); UV (100 J/m^2, 4 h); Cisplatin (33 μM, 4 h). Quantification of cells with >10 TRAIP/γH2AX overlapping foci (A; right panel) or relative nucleolar/cytoplasmic S9.6 signal intensity (B; right panel) are shown. Results (mean ± SEM) were calculated from three independent experiments. *P < 0.05, **P < 0.01 versus Mock; (**C**) I-PpoI-induced rDNA damage triggers nucleolus-nucleoplasm shuttling of TRAIP. Cells stably expressing TRAIP-Flag or its PCNA binding-defective mutant (TRAIP-PIP*-Flag) were induced with Shield-1 (0.5 μM) and 4-OHT (2 μM) to express the I-PpoI endonuclease. Cells were subsequently fixed after 4 h and were processed for immunostaining experiments as in (A). Percentage of cells (mean ± SEM) with nucleolar TRAIP-Flag signal is calculated from three independent experiments, n > 100; (**D**) TRAIP-Flag expressing cells were subjected to pre-treatment of RNA polymerase inhibitors, including Actinomycin D (ActD; 0.05 μg/ml), α-Amanitin (50 μg/ml), DRB (100 μM) and CX5461 (1.42 μM), and were processed for immunostaining experiments as in (A). Quantification of cells with nucleolar TRAIP signal or S9.6 signal are shown (bottom panel). Results (mean ± SEM) were derived from three independent experiments, n > 100. *P < 0.05, **P < 0.01 versus Mock; (**E**) TRAIP-Flag expressing cells permeabilized using 0.5% Triton X-100 solution were treated with DNase I (0.5 U/μl), RNase A (1 mg/ml) or mock before they were fixed and processed for immunostaining experiments using indicated antibodies. Percentage of cells showing either Nucleolin or TRAIP localization in the nucleoli are shown. Experiments were repeated three times and >100 cells were analyzed.

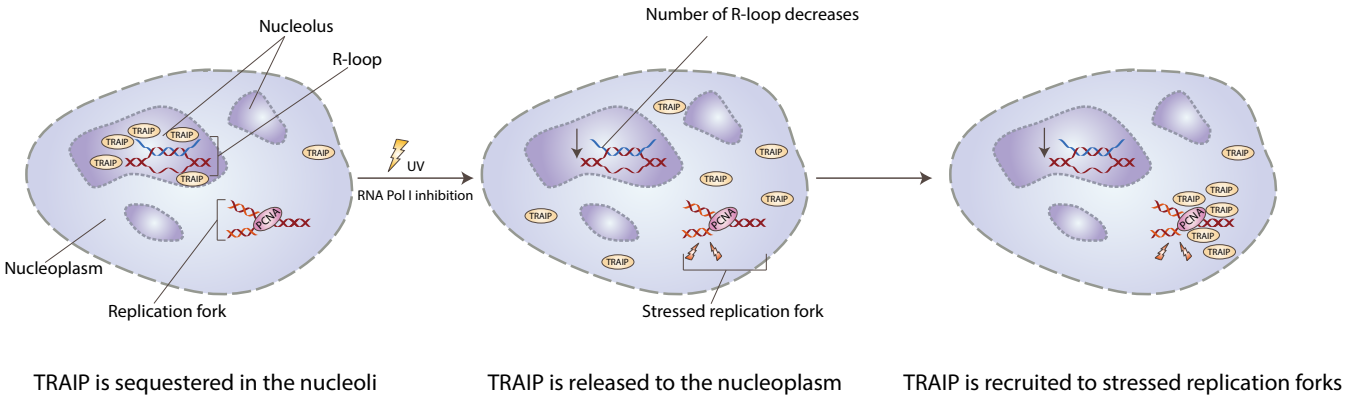

Figure 7. Working model. Schematic depicting a two-step mechanism that drives the intracellular trafficking of TRAIP in response to UV irradiation. TRAIP is associated with nucleolar R-loops in unperturbed cells. Upon UV irradiation, nucleolar R-loops are dissolved, which triggers the release of TRAIP from the nucleoli. TRAIP subsequently concentrates at UV-stressed replication forks via its PCNA-binding PIP motif.

TRAIP-Flag enrichment at γH2AX foci (Figure 6A), it did not noticeably affect the sub-cellular localization of other nucleolar proteins, including Ki-67 and Nucleolin (Supplementary Figure S4A–C).

We also specifically targeted the nucleoli chromatin using the I-PpoI endonuclease, which cuts a rare sequence at the 45S rDNA loci (43). We reasoned that DNA double-strand breaks at the rDNA loci should impair rDNA transcription and compromise R-loop structures, which may in turn lead to TRAIP release from the nucleoli. Accordingly, induction of I-PpoI led to the accumulation of γH2AX at the nucleoli periphery, an observation consistent with the idea that damaged rDNA relocalizes for repair processes (Figure 6C) (3). In support of the idea that TRAIP retention in the nucleoli is coupled to ongoing rDNA transcription, TRAIP became excluded from the nucleoli in I-PpoI-expressing cells in a manner that did not require its PIP motif (Figure 6C).

To further examine if R-loops may be important in sequestering TRAIP in the nucleoli, we pre-treated cells with a panel of rDNA transcription inhibitors, including the DNA intercalating agent Actinomycin D (ActD), the RNA polymerase II inhibitors α-Amanitin and DRB, and the RNA polymerase I inhibitor CX5461. Importantly, we found that Actinomycin D and CX5461 efficiently suppressed nucleolar S9.6 signals, and were coupled with TRAIP exclusion from the nucleolar compartments (Figure 6D). On the other hand, α-Amanitin and DRB treatments had modest effects on R-loop dissolution in the nucleoli, which correlated with more subtle effects on TRAIP migration out from the nucleoli (Figure 6D). These data suggest that TRAIP may anchor, either directly or indirectly, to R-loops in the nucleoli. Consistently, we found that nuclease treatment prior to cell fixation not only attenuated nucleolar S9.6 signals (Supplementary Figure S5), but also released TRAIP from the nucleoli (Figure 6E), supporting the idea that TRAIP retention in the nucleoli may be coupled to ongoing rRNA synthesis and R-loop structures (Figure 7).

DISCUSSION

The Seckel syndrome protein TRAIP has emerged as a pivotal component of the mammalian replicative stress response. TRAIP responds to UV irradiation, and accumulates at stressed replication forks via its ability to interact with the DNA replication factor PCNA (22,25). Notably, because TRAIP concentrates in the nucleoli, delineating how UV triggers its release from the nucleoli is key to understanding its regulation in the protection of genome integrity, especially as this may represent a rate-limiting step that underlies its responsiveness to replicative stress. In this study, we provide several lines of evidence to support a two-step mechanism that orchestrates TRAIP trafficking across the nuclear sub-compartments in response to UV irradiation (Figure 7). Our data suggest that TRAIP associates with R-loops in the nucleoli, and that its release is coupled to dampened rDNA synthesis and R-loop dissolution.

Although an early study reported that ectopically-expressed TRAIP forms nuclear puncta (26), it is now established that TRAIP resides predominantly in the nucleoli, and that epitope-tagging TRAIP at its N terminus, but not its C-terminus, precluded ectopically-expressed TRAIP proteins to properly localisze in the nuclear subcompartment (23,25,27,44). These pieces of circumstantial evidence suggested that TRAIP may target the nucleoli via its N-terminal domain(s). In support of this idea, not only do mutations that inactivate its RING domain (i.e. C7A, R18C and RING deletion) mis-localized TRAIP from the nucleoli (Figure 3F), deleting the Coiled-coil and Zipper domains also impaired its ability to concentrate in the nucleoli (Figure 3B-C). While TRAIP Zipper was sufficient to localize in the nucleoli (Figure 3D and E), the idea that the E3 ligase signature motif on the TRAIP polypeptide may also serve a specialized role to mediate its concentration in the nucleoli is supported not only by our indirect immunofluorescence experiments (Figure 3D and E), but also by our RING domain swapping experiment where we found that the RING derived from a non-nucleolar protein (i.e. RNF168) did not fully support its nucleolar localization (Figure 3G–I). The idea that TRAIP RING and Zipper domains synergize to mediate nucleolar enrichment of TRAIP is further supported by our photo-bleaching experiments, which revealed substantially shorter residence of TRAIP RING and Zipper domains in the nucleoli as compared to full-length TRAIP-GFP proteins (Figure 4). Together, these data raise

the exciting possibility that TRAIP may engage in multivalent interactions with various nucleolar components. While the identities of these nucleolar components remain to be identified, they likely encompass both DNA–RNA structures and core nucleolar proteins, the latter of which is supported by previous analyses of TRAIP protein complexes (25).

Our observations that R-loop dissolution closely correlated with redistribution of TRAIP into the nucleoplasm prompted us to formulate a working model in which DNA/RNA hybrid structures may represent one of the key nucleolar determinants that anchor TRAIP in the membrane-less organelle (Figure 7). Indeed, cell pretreatment with both DNase and RNase effectively released TRAIP from the nucleoli (Figure 6E), as were nucleolar S9.6 signals (Supplementary Figure S5). Interestingly, UV-induced release of TRAIP from the nucleoli is effected independently of the master DNA damage response kinases ATM and ATR (Figure 5). Given that chemical inhibition of ATM and ATR did not noticeably affect the UV-induced dissolution of R-loops (Figure 5D and E), it is tempting to speculate that R-loop dissolution in the nucleoli may be regulated by a distinct, yet unidentified, mechanism(s). While it remains to be seen how R-loop processing is coupled to UV responses, and whether TRAIP enrichment in the nucleoli may have additional function that directly contributes to cell proliferation, our data support the idea that the nucleoli serve as stress sensors, and by regulating protein flux in and out of the nuclear sub-compartments, play key roles in cell proliferation.

Human TRAIP mutations are associated with microcephalic primordial dwarfism (24). Interestingly, we found that both clinically-derived TRAIP mutations (i.e. R18C and R185X) perturbed its subcellular localization (Figure 1E), highlighting the importance of protein compartmentalization in supporting cell and organismal development. While a more detailed understanding of how TRAIP protects genome integrity awaits further work, our study has uncovered a bipartite strategy that governs the swift intracellular trafficking of a DNA damage response protein in the mammalian UV response.

SUPPLEMENTARY DATA

Supplementary Data are available at NAR Online.

ACKNOWLEDGEMENTS

We thank Dr Roger Greenberg for generous sharing of the I-PpoI expression plasmid. We also acknowledge the technical advice and support from Dr Jing Guo and Faculty Core Facility (The University of Hong Kong) with imaging analyses.

FUNDING

Research Grants Council Hong Kong [17102017, C7007-17GF to M.H.]. Funding for open access charge: Research Grants Council Hong Kong.
Conflict of interest statement. None declared.

REFERENCES

1. Raska,I., Shaw,P.J. and Cmarko,D. (2006) Structure and function of the nucleolus in the spotlight. *Curr. Opin. Cell Biol.*, **18**, 325–334.
2. Boulon,S., Westman,B.J., Hutten,S., Boisvert,F.M. and Lamond,A.I. (2010) The nucleolus under stress. *Mol. Cell*, **40**, 216–227.
3. Larsen,D.H. and Stucki,M. (2016) Nucleolar responses to DNA double-strand breaks. *Nucleic Acids Res.*, **44**, 538–544.
4. Boisvert,F.M., van Koningsbruggen,S., Navascues,J. and Lamond,A.I. (2007) The multifunctional nucleolus. *Nat. Rev. Mol. Cell Biol.*, **8**, 574–585.
5. van Sluis,M. and McStay,B. (2017) Nucleolar reorganization in response to rDNA damage. *Curr. Opin. Cell Biol.*, **46**, 81–86.
6. Lindstrom,M.S., Jurada,D., Bursac,S., Orsolic,I., Bartek,J. and Volarevic,S. (2018) Nucleolus as an emerging hub in maintenance of genome stability and cancer pathogenesis. *Oncogene*, **37**, 2351–2366.
7. Pelava,A., Schneider,C. and Watkins,N.J. (2016) The importance of ribosome production, and the 5S RNP-MDM2 pathway, in health and disease. *Biochem. Soc. Trans.*, **44**, 1086–1090.
8. Tsai,R.Y. and Pederson,T. (2014) Connecting the nucleolus to the cell cycle and human disease. *FASEB J.*, **28**, 3290–3296.
9. Stark,L.A. and Taliansky,M. (2009) Old and new faces of the nucleolus. Workshop on the nucleolus and disease. *EMBO Rep.*, **10**, 35–40.
10. Farley-Barnes,K.I., McCann,K.L., Ogawa,L.M., Merkel,J., Surovtseva,Y.V. and Baserga,S.J. (2018) Diverse regulators of human ribosome biogenesis discovered by changes in nucleolar number. *Cell Rep.*, **22**, 1923–1934.
11. Buchwalter,A. and Hetzer,M.W. (2017) Nucleolar expansion and elevated protein translation in premature aging. *Nat. Commun.*, **8**, 328.
12. de Los Santos-Velazquez,A.I., de Oya,I.G., Manzano-Lopez,J. and Monje-Casas,F. (2017) Late rDNA condensation ensures timely Cdc14 release and coordination of mitotic exit signaling with nucleolar segregation. *Curr. Biol.*, **27**, 3248–3263.
13. Tiku,V., Jain,C., Raz,Y., Nakamura,S., Heestand,B., Liu,W., Spath,M., Suchiman,H.E.D., Muller,R.U., Slagboom,P.E. *et al.* (2016) Small nucleoli are a cellular hallmark of longevity. *Nat. Commun.*, **8**, 16083.
14. Andersen,J.S., Lam,Y.W., Leung,A.K., Ong,S.E., Lyon,C.E., Lamond,A.I. and Mann,M. (2005) Nucleolar proteome dynamics. *Nature*, **433**, 77–83.
15. Andersen,J.S., Lyon,C.E., Fox,A.H., Leung,A.K., Lam,Y.W., Steen,H., Mann,M. and Lamond,A.I. (2002) Directed proteomic analysis of the human nucleolus. *Curr. Biol.*, **12**, 1–11.
16. Carmo-Fonseca,M., Mendes-Soares,L. and Campos,I. (2000) To be or not to be in the nucleolus. *Nat. Cell Biol.*, **2**, E107–E112.
17. Martin,R.M., Ter-Avetisyan,G., Herce,H.D., Ludwig,A.K., Lattig-Tunnemann,G. and Cardoso,M.C. (2015) Principles of protein targeting to the nucleolus. *Nucleus*, **6**, 314–325.
18. Scott,M.S., Boisvert,F.M., McDowall,M.D., Lamond,A.I. and Barton,G.J. (2010) Characterization and prediction of protein nucleolar localization sequences. *Nucleic Acids Res.*, **38**, 7388–7399.
19. Emmott,E. and Hiscox,J.A. (2009) Nucleolar targeting: the hub of the matter. *EMBO Rep.*, **10**, 231–238.
20. Yuan,Y.F., Ren,Y.X., Yuan,P., Yan,L.Y. and Qiao,J. (2016) TRAIP is involved in chromosome alignment and SAC regulation in mouse oocyte meiosis. *Sci. Rep.*, **6**, 29735.
21. Soo Lee,N., Jin Chung,H., Kim,H.J., Yun Lee,S., Ji,J.H., Seo,Y., Hun Han,S., Choi,M., Yun,M., Lee,S.G. *et al.* (2016) TRAIP/RNF206 is required for recruitment of RAP80 to sites of DNA damage. *Nat. Commun.*, **7**, 10463.
22. Hoffmann,S., Smedegaard,S., Nakamura,K., Mortuza,G.B., Raschle,M., Ibanez de Opakua,A., Oka,Y., Feng,Y., Blanco,F.J., Mann,M. *et al.* (2016) TRAIP is a PCNA-binding ubiquitin ligase that protects genome stability after replication stress. *J. Cell Biol.*, **212**, 63–75.
23. Chapard,C., Meraldi,P., Gleich,T., Bachmann,D., Hohl,D. and Huber,M. (2014) TRAIP is a regulator of the spindle assembly checkpoint. *J. Cell Sci.*, **127**, 5149–5156.
24. Harley,M.E., Murina,O., Leitch,A., Higgs,M.R., Bicknell,L.S., Yigit,G., Blackford,A.N., Zlatanou,A., Mackenzie,K.J., Reddy,K. *et al.* (2016) TRAIP promotes DNA damage response during genome

replication and is mutated in primordial dwarfism. *Nat. Genet.*, **48**, 36–43.
25. Feng,W., Guo,Y., Huang,J., Deng,Y., Zang,J. and Huen,M.S. (2016) TRAIP regulates replication fork recovery and progression via PCNA. *Cell Discov.*, **2**, 16016.
26. Merkle,J.A., Rickmyre,J.L., Garg,A., Loggins,E.B., Jodoin,J.N., Lee,E., Wu,L.P. and Lee,L.A. (2009) no poles encodes a predicted E3 ubiquitin ligase required for early embryonic development of Drosophila. *Development*, **136**, 449–459.
27. Wallace,H.A., Merkle,J.A., Yu,M.C., Berg,T.G., Lee,E., Bosco,G. and Lee,L.A. (2014) TRIP/NOPO E3 ubiquitin ligase promotes ubiquitylation of DNA polymerase eta. *Development*, **141**, 1332–1341.
28. Raschle,M., Smeenk,G., Hansen,R.K., Temu,T., Oka,Y., Hein,M.Y., Nagaraj,N., Long,D.T., Walter,J.C., Hofmann,K. *et al.* (2015) DNA repair. Proteomics reveals dynamic assembly of repair complexes during bypass of DNA cross-links. *Science*, **348**, 1253671.
29. Wanjuan,F., Yingying,G., Jun,H., Yiqun,D., Jianye,Z. and Michael Shing-Yan,H. (2016) TRAIP regulates replication fork recovery and progression via PCNA. *Cell Discov.*, **2**, 16016.
30. Huen,M.S., Grant,R., Manke,I., Minn,K., Yu,X., Yaffe,M.B. and Chen,J. (2007) RNF8 transduces the DNA-damage signal via histone ubiquitylation and checkpoint protein assembly. *Cell*, **131**, 901–914.
31. McKinney,S.A., Murphy,C.S., Hazelwood,K.L., Davidson,M.W. and Looger,L.L. (2009) A bright and photostable photoconvertible fluorescent protein. *Nat. Methods*, **6**, 131–133.
32. Yang,K., Wang,M., Zhao,Y., Sun,X., Yang,Y., Li,X., Zhou,A., Chu,H., Zhou,H., Xu,J. *et al.* (2016) A redox mechanism underlying nucleolar stress sensing by nucleophosmin. *Nat. Commun.*, **7**, 13599.
33. Chen,D. and Huang,S. (2001) Nucleolar components involved in ribosome biogenesis cycle between the nucleolus and nucleoplasm in interphase cells. *J. Cell Biol.*, **153**, 169–176.
34. Maria,C.-F., Luís,M.-S. and Isabel,C. (2000) To be or not to be in the nucleolus. *Nat. Cell Biol.*, **2**, E107.
35. Sean,A.M., Christopher,S.M., Kristin,L.H., Michael,W.D. and Loren,L.L. (2009) A bright and photostable photoconvertible fluorescent protein. *Nat. Methods*, **6**, 131.
36. Chen,J., Feng,W., Jiang,J., Deng,Y. and Huen,M.S. (2012) Ring finger protein RNF169 antagonizes the ubiquitin-dependent signaling cascade at sites of DNA damage. *J. Biol. Chem.*, **287**, 27715–27722.
37. Shiloh,Y. (2003) ATM and related protein kinases: safeguarding genome integrity. *Nat. Rev. Cancer*, **3**, 155–168.
38. Cimprich,K.A. and Cortez,D. (2008) ATR: an essential regulator of genome integrity. *Nat. Rev. Mol. Cell Biol.*, **9**, 616–627.
39. Curtin,N.J. (2012) DNA repair dysregulation from cancer driver to therapeutic target. *Nat. Rev. Cancer*, **12**, 801–817.
40. Bhatia,V., Barroso,S.I., García-Rubio,M.L., Tumini,E., Herrera-Moyano,E. and Aguilera,A. (2014) BRCA2 prevents R-loop accumulation and associates with TREX-2 mRNA export factor PCID2. *Nature*, **511**, 362.
41. Garcia-Rubio,M.L., Perez-Calero,C., Barroso,S.I., Tumini,E., Herrera-Moyano,E., Rosado,I.V. and Aguilera,A. (2015) The Fanconi Anemia pathway protects genome integrity from R-loops. *PLoS Genet.*, **11**, e1005674.
42. Hodroj,D., Recolin,B., Serhal,K., Martinez,S., Tsanov,N., Abou Merhi,R. and Maiorano,D. (2017) An ATR-dependent function for the Ddx19 RNA helicase in nuclear R-loop metabolism. *EMBO J.*, **36**, 1182–1198.
43. Harding,S.M., Boiarsky,J.A. and Greenberg,R.A. (2015) ATM dependent silencing links nucleolar chromatin reorganization to DNA damage recognition. *Cell Rep.*, **13**, 251–259.
44. Zhou,Q. and Geahlen,R.L. (2009) The protein-tyrosine kinase Syk interacts with TRAF-interacting protein TRIP in breast epithelial cells. *Oncogene*, **28**, 1348–1356.